CARPATHIAN J. MATH.
Volume **41** (2025), No. 2,
Pages 371-391

Online version at `https://www.carpathian.cunbm.utcluj.ro/`
ISSN 1584-2851 (Print edition); ISSN 1843-4401 (Electronic)
DOI: https://doi.org/10.37193/CJM.2025.02.07

Geometry of C_{32} cyclic polyyne and some of its clusters

LORENTZ JÄNTSCHI[1] AND LAVINIA-LORENA PRUTEANU[2]

ABSTRACT. Cyclic chemical compounds can form clusters. Cyclic C_{32} polyyne is considered here. For a system in which 4 C_{32} rings cross independently of each other, a fifth C_{32} ring has been found a minimal energy conformation that favors the recursion of this structural unit in the 3 dimensions of space. C_{32} polyyne rings have been used to form linked clusters when geometry of C_{32} reveals that are no steric impediments in crossing it in a 4 pointed star arrangement. Larger clusters have been derived by recursion having the crossing star pattern. Shape of the cluster was found to be approximated by a bifrustum. The analysis allowed to estimate a limit value (crystal-like) of 502.56 kg/m^3 for the density of the cluster, with even smaller values for smaller clusters. Energy build analysis has shown that almost entirely the energy of the cluster is given by the internal forces connecting the atoms in the rings and only less than 0.0003% can be attributed to the intermolecular forces between the rings.

1. INTRODUCTION

We must go back till the discovery of the chemical structure [47] to find the first studies on carbon–carbon chains [48]. Carbon is by far the most readily element in catenation but should be acknowledged here that other elements are bridging long chains of monomers or molecules. Here are some classical examples: hydrogen in hydrogen bonds bridging water molecules and DNA bases, oxygen bridging monosaccharides in polycarbohydrates, sulphur bridging polyisoprene chains sections in rubber. Other examples include oxygen and phosphorus in phosphodiesters, oxygen and silicium in silicones, oxygen, silicium and aluminum in zeolites, and the complexity of repeating unit can go on and on.

The number of isomers of branched chains of carbon is impressive. A000602 [74] integer sequence lists their numbers when ignoring stereoisomers and A000628 [75] when stereoisomers are considered.

If the formation of linear or branched chains is one of the tools with which nature organizes the higher levels of matter, then the second tool is the formation of cycles. Looking at the number of distinct bonds, carbon can form 2, 3 or 4, in which cases the natural angle between them is $\arccos(-1)$, $\arccos(-1/2)$, and $\arccos(-1/3)$ respectively. Apeirogon ($n = \infty$), heptagon ($n = 7$), hexagon ($n = 6$), and pentagon ($n = 5$), are the polygons with closest angles ($\frac{n-2}{n}\pi$; π, $5\pi/7$, $4\pi/6$, and $3\pi/5$) to these angles (π, $2\pi/3$, and $14\pi/23$), which explains the tendency of carbon to form mostly rings of 5 and 6 atoms, but also predicts the stability for heptagons, long chains and large rings.

Another way of organization is the formation of molecular aggregates. They can be formed mainly by establishing hydrogen bonds, but other forces (such as van der Waals forces) contribute significantly to the formation of complex molecular aggregates.

Molecular topology [20] addresses these topics in the context of characterization and classification of molecular structures. The preferred tool of molecular topology is unweighted and unoriented graphs, in which all heavy atoms (only hydrogen is light; the

---

Received: 01.05.2024. In revised form: 09.09.2024. Accepted: 14.09.2024
2020 *Mathematics Subject Classification.* 81V99, 92E10, 14J29, 14J33.
Key words and phrases. *polyynes, clusters, nets, symmetry, stability.*
Corresponding author: Lavinia-Lorena Pruteanu; pruteanulavinia@gmail.com

other atoms are heavy) are undistinguishable. An important result in relation to the representation of molecules in the form of molecular graphs is that the number of attached hydrogen atoms is always a recoverable information from the heavy atoms graph representation of the molecule. Thus, if n_{C}, n_{N}, n_{O} and n_{H} are the number of atoms of carbon, nitrogen, oxygen and hydrogen, and b the number of bonds between heavy atoms (numbered here conventionally by multiplying with the bond order), then:

$$4n_{\mathrm{C}} + 3n_{\mathrm{N}} + 2n_{\mathrm{O}} = n_{\mathrm{H}} + 2b. \tag{1.1}$$

Eq. (1.1) become $2n_{\mathrm{C}} = b$ for compounds made only from carbon atoms, such is the case for cyclic polyynes (ex.: C_{32} here, C_{28} in [79]) and cumulenes (ex: C_{26} in [45]).

Molecular knots is a special arrangement within molecular aggregates - and cyclic C_{32} polyyne clusters falls in - formation of clusters without implying or implicitly assuming the existence of forces that hold the molecules together in the cluster, but whose presence can actually stabilize the molecules constitutive of the cluster. Catenanes, containing two or more intertwined rings, are a special case of knots which gain much more interest since the preparation of the first [19].

Here the construction of an interlinked cyclo[32]carbon (or C_{32} cyclic polyyne) network is analyzed. The repetitive basic unit is a C_{32} ring that is intersected by 4 other C_{32} rings located in a plane perpendicular to it and in which are twisted to each other at 90 °.

2. CARBON-BASED ASSEMBLIES

As a part of their applications as molecular wires linear polyynes and cumulenes have been studied in detail and [14] review covers at least in part this area of interest. Topologically, cumulenes contain sequences of carbon-carbon double bonds, while polyynes alternate single and triple bonds. A linear chain may be hydrogen capped (Tab. 1).

TABLE 1. Hydrogen capped linear polyynes and cummulenes.

Nº	**Molecular formula**	**Rational formula**	**Type**
1	C_nH_2	$HC{\equiv}C{-}\cdots C\cdots{-}C{\equiv}CH$	polyyne
2	C_nH_4	$H_3C{-}C{\equiv}\cdots C\cdots{-}C{\equiv}CH$	polyyne
3	C_nH_4	$H_2C{=}C{=}\cdots C\cdots{=}C{=}CH_2$	cumulene
4	C_nH_4	$HC{\equiv}C{-}\cdots C\cdots{\equiv}C{-}CH_3$	polyyne
5	C_nH_6	$H_3C{-}C{\equiv}\cdots C\cdots{\equiv}C{-}CH_3$	polyyne

Molecules 2 and 4 are identical due to the isomorphism of the representation

If the olyyne is bent to form a ring, then the limit conformations are only two (Tab. 2).

TABLE 2. Conformations of cyclic polyynes and cummulenes.

Nº	**Molecular formula**	**Structural formula**	**Type**
1	C_n	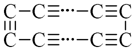	polyyne
2	C_n	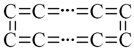	cumulene

The generic name of C_n is cyclo[n]carbon; n must be a multiple of 2

Different studies have investigated cyclic polyynes and cumulenes of different sizes. A cyclo-carbon C_n is a polyyne if $n = 4k$ (k = 2, 3, ...) and is a cumulene if $n = 4k + 2$ (k = 2, 3, ...). Literature reports are summarized in Tab. 3.

TABLE 3. Some cyclo[n]carbons in increasing size.

Size (n)	**Cumulene studies**		**Size** (n)	**Polyyne studies**	
6	C_6	[65, 66, 44]	8	C_8	[61, 66, 44]
10	C_{10}	[61, 66, 44]	12	C_{12}	[66, 44, 37]
14	C_{14}	[66, 44, 37]	16	C_{16}	[66, 44, 37]
18	C_{18}	[66, 44, 37, 24, 15]	20	C_{20}	[66, 44, 24, 53]
22	C_{22}	[66, 44, 24, 53, 15]	24	C_{24}	[66, 44, 24, 53, 46]
26	C_{26}	[66, 44, 24, 53, 15]	28	C_{28}	[66, 44, 24]
30	C_{30}	[66, 44, 24, 15]	32	C_{32}	[66, 44, 24] & this study

n must be a multiple of 2

Calculations on cyclo[n]carbon proved that they would be more stable than linear chains for $n \geq 10$ [37], and from $n = 16$ quickly approach the minimum energy state [39], but should be kept in mind that from $n = 20$ the C_n fullerenes also stabilizes [81, 38].

Among chemical compounds sharing the same molecular formula is not uncommon the rearrangement of the bonds and transition from one topology to another (called tautomerism). C_{32} fullerene is a rearrangement of the bonds from cyclic C_{32} polyyne. Referring C_{32} fullerenes, there are exactly 6 isomers of C_{32} fullerene (Fig. 1).

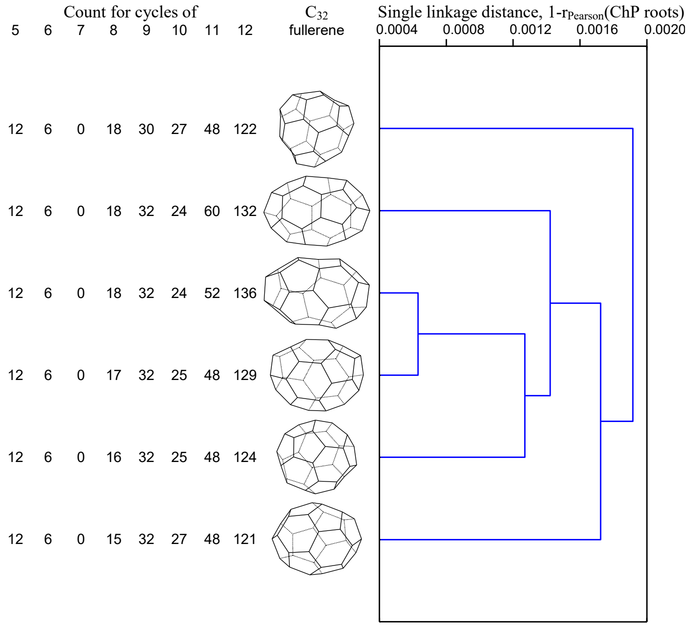

Count for cycles of 5	6	7	8	9	10	11	12
12	6	0	18	30	27	48	122
12	6	0	18	32	24	60	132
12	6	0	18	32	24	52	136
12	6	0	17	32	25	48	129
12	6	0	16	32	25	48	124
12	6	0	15	32	27	48	121

FIGURE 1. C_{32} fullerenes, differentiation on cycles of length at most 12 and clustering on the correlation of characteristic polynomial (ChP) roots

Moreover, the connection between fullerenes and cyclo[n]carbon is strong. Thus, cyclization of polyynic and cumulenic carbon chains was observed at laser vaporization of graphite as secondary product in the synthesis of fullerenes in [36] for $22 \leq n \leq 46$.

Euler's formula [23] for a convex polyhedron with n vertices, E edges, and F faces is:

$$n - E + F = 2 \tag{2.2}$$

An important property was established [85]: If a convex polyhedron the faces have only 5 vertices (pentagons) or 6 vertices (hexagons), then in Eq. (2.2), n must be even, must be exactly 12 pentagons and $n/2 - 10$ hexagons. All topologies given in Fig. 1 follows this rule. On should note that Fig. 1 isomers are very similar topologically one with each other: all have exactly 12 cycles of 5 and 6 cycles of 6 (as faces and as smallest set of smallest rings) and the difference between them is made only at the arrangement of those rings. More, the series of characteristic polynomial roots values are highly correlated (the lowest correlation is 0.994 and the highest is 0.999).

The structure and bonding of C_{32} carbon clusters has been the subject of theoretical investigation in [41], was found as a secondary product in [21], and a synthetic route to tris(3,5-di-t-butylphenyl)methyl (Tr) capped polyyne ($n = 32$ at entry 1 in Tab. 1) has been reported in [18]. In the same work [18] the HOMO-LUMO bandgap of Tr capped C_{32} polyyne has been estimated at about 89% of the bandgap of the hypothetic carbine (C_∞, $E_{\mathrm{LUMO}} - E_{\mathrm{HOMO}}$ = 2.56 eV).

The interlocking of the chains stabilizing the molecules as a cluster is supported by [76, 77, 53], while concurrent processes are of polymerization [40].

Experimental data for electronic spectra of hydrogen capped linear polyynes and cumulenes C_nH_4 are readily in the literature till $n = 10$ in [50], $n = 24$ in [28], $n = 26$ in [63], and $n = 44$ in [18].

The proper name for C_{32} cyclic polyyne is cyclic hexadecayne since it have exactly 16 single and 16 triple bonds. Crossing (or interlinking) of a cyclic hexadecayne by other 4 cyclic hexadecaynes clearly defines a polycatenane, namely a [5]catenane [68], and cyclo[32]carbon[5]catenane as family name seems reasonable.

3. Mathematical modeling

3.1. **C_{32} topology.** Cyclo[32]carbon (using the nomenclature defined in [68]) is made entirely from carbon atoms in which are alternating single and triple bonds. This feature allows a simplified representation as a graph (Fig. 2). As previous studies have shown, it is expected to be a planar structure which gain more stability from its symmetry.

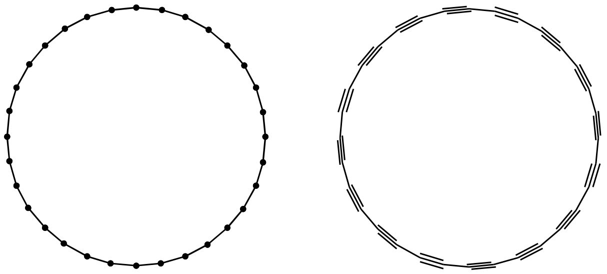

atoms representation (dots, vertices)

bonds representation (lines, edges)

Figure 2. C_{32} cyclic polyyne as a graph

The parameters characterizing the structure are the bond lengths, which along with the angles completely defines the structure in internal coordinates. Z-matrix [6] formalism is given in Fig. 3.

$$\begin{array}{cccccccc}
1 & \text{C} & & & & & & \\
2 & \text{C} & 1 & a_{s(2)} & & & & \\
3 & \text{C} & 2 & a_{s(3)} & 1 & a_2 & & \\
 & & & & \ldots & & & \\
i & \text{C} & i-1 & a_{s(i)} & i-2 & a_2 & i-3 & a_3 \\
 & & & & \ldots & & & \\
n & \text{C} & 1 & a_{s(1)} & 2 & a_2 & 3 & a_3
\end{array}$$

FIGURE 3. C_{32} cyclic polyyne in Z-matrix internal coordinates ($n = 32$)

In Fig. 3, a parameter is constant ($a_3 = 0.0\ ^\circ$) while the other (a_2) depend on the value of n ($n = 32$ for C_{32}) and i (from 1 to $n-1$):

$$a_2 = 180\frac{n-2}{n}\ ^\circ \tag{3.3}$$

$$s(i) = \frac{1-(-1)^i}{2} \text{ for } i = 1, 2, ..., n-1 \tag{3.4}$$

In Eq. (3.3) a_2 is defining an angle which increases with n, while in Eq. (3.4) $s(i)$ defines an alternating function $(s(1) = 1, s(2) = 0, ...)$ having thus two variable parameters (a_0 and a_1).

The distances a_0 and a_1 (usually given in Å in Z-matrix [6] files) are the subject of molecular geometry optimization (by minimizing the energy of the molecule), which solves a problem of localization.

3.2. **Numerical method.** Localization (of the atoms inside the molecule) is usually solved via the conservation of the total energy for an isolated system and respectively the quantification of the variation of the total energy for a closed system in (quantified) exchange with its environment. Under these principles, the change in time of the total energy in the presence of an outside field U (produced outside of the system, considered uniformly distributed in the closed system, time dependent) in a closed system of k particles (characterized by their spatial positions $\vec{r_1} = \vec{r_1}(t), ..., \vec{r_k} = \vec{r_k}(t)$) are expressed through the Schrödinger's equation [69]:

$$\hat{H}\Psi(\vec{r}_1, ..., \vec{r}_k, t) = i\hbar\frac{\partial}{\partial t}\Psi(\vec{r}_1, ..., \vec{r}_k, t) + U(t) \tag{3.5}$$

$$\rho(\vec{r}_1, ..., \vec{r}_k, t) = |\Psi(\vec{r}_1, ..., \vec{r}_k, t)|^2 \tag{3.6}$$

where $\hat{H}$ is the Hamiltonian (providing the total energy of the system), i the imaginary unit ($\sqrt{-1}$), $\hbar$ is the reduced Planck constant ($\hbar = \frac{h}{2\pi}$, $h = 6.62607015 \times 10^{-34}$ kg $\cdot$ m $\cdot$ rad $\cdot$ s^{-1}), Ψ is the wavefunction (a complex-valued function building up the probability density - function ρ from Eq. (3.6) - and localizing thus the system), and for simplification the spin effects were neglected.

Eq. (3.5) admits as solutions time independent wave functions called standing waves, associated with stationary states. For a system whose Hamiltonian has no explicit time dependence, it makes sense to try and find stationary states, for which the time evolution is given by an explicit separable function (Ψ_t in Eq. (3.7)):

$$\Psi(\vec{r}_1, ..., \vec{r}_k, t) = \Psi_s(\vec{r}_1, ..., \vec{r}_k)\Psi_t(t) \tag{3.7}$$

where Ψ_s characterizes a stationary state and simplifies the solving of Eq. (3.5) for any state.

However, direct solving of Eq. (3.5) is still a challenge (even numerical), so a series of approximations are in practice applied. Born-Oppenheimer approximation [13] stiffens the nucleuses allowing the separation of their functions - Eq. (3.8):

$$\Psi_s(\vec{r}_1, ..., \vec{r}_k) = \Psi_n(\vec{r}_1, ..., \vec{r}_{k_n}) \cdot \Psi_e(\vec{r}_1, ..., \vec{r}_{k_e}) \tag{3.8}$$

where Ψ_n is the wave function of k_n nucleons and Ψ_e is the wave function of k_e electrons.

To accurately approximate the energy of the system, a series of models (including Bohr-Sommerfeld, Thomas-Fermi, Thomas-Fermi-Dirac, and Thomas-Fermi-Dirac-Weizsäcker) and corrections were proposed [7]. Even so, Eq. (3.5) is accessible for real cases only in the context of certain simplifications [22, 11].

Hartree-Fock (HF) method ([29, 30, 25, 26]) separates the Ψ_n and Ψ_e wavefunctions by their variables such that this separation to be the simplest one keeping the antisymmetry at permuting of the variables. Slater [72] express Ψ_E as a determinant (of k_e wavefunctions for k_e electrons) and as a permanent (of k_n wavefunctions for k_n nucleons):

$$\Psi_e(\vec{r}_1, ..., \vec{r}_k) = \text{Imm}_\lambda \begin{pmatrix} \psi_1(\vec{r}_1) & ... & \psi_{n_e}(\vec{r}_1) \\ ... & ... & \\ \psi_1(\vec{r}_{n_e}) & ... & \psi_{n_e}(\vec{r}_{n_e}) \end{pmatrix} \tag{3.9}$$

where Imm_λ is the immanant [55] and $\text{Imm}_{-1} = \det$ (determinant, when $\lambda = -1$) and $\text{Imm}_1 = \text{perm}$ (permanent, when $\lambda = 1$).

Again Slater [73] proposed the localization of the electrons in the orbitals with a function having as radial part a Laplace distribution function (named STO, Eq. (3.10)), which was later replaced [31] with sums of Gauss distribution functions (Gaussians, named STO-nG or GTO, in Eq. (3.11)).

$$\psi_{e,\text{STO}}(r; Z, \alpha, \beta) = r^{\alpha-1} e^{\frac{(Z-\beta)r}{\alpha}} \tag{3.10}$$

where Z, α and β constants depending on the atom, its population with electrons, electronic shell and group (see [73] for numeric values).

$$\psi_{e,\text{STO-}n\text{G}}(r; \{\gamma_i, \theta_i\}_{i=1,...,4}, \{\delta_k, \epsilon_k\}_{1,...,n}) = \sum_{k=1}^{n} \delta_k r^{\gamma_i} e^{-\epsilon_k r^2} \cos(\theta_i) \tag{3.11}$$

where γ_k and θ_k for $i = 1, ..., 4$ constants depending on the type of the orbital approximated (s, p, d, f) and δ_k and ϵ_k for $k = 1, ..., n$ constants depending also on the number of the basic functions used (n).

Hohenberg and Kohn have shown [34] that in the ground state Ψ_e is a uniquely determined functional which may be expressed depending on the electronic density alone (ρ in Eq. (3.12)).

$$\Psi_e(\vec{r}_1, ..., \vec{r}_k) = \Psi_{\text{HK}}(\rho(\vec{r}_1, ..., \vec{r}_k)) \tag{3.12}$$

where Ψ_{HK} the functional featuring the desired property (HK, Eq. (3.12)). The use of a fictive system with no interactions and with movement of the electrons in the presence of an potential of a single particle to reproduce the same fundamental state with the real system in which the interaction is present has been later then proposed [51]. The main advantage of this approach is that in the absence of interactions, the wavefunction is separable in its variables [35].

3.3. **Software.** Several molecular modeling software can be used to localize the atoms in molecules implying different implementations of the Eq. (3.5)-(3.12). The use of a molecular modeling software usually requires choosing of a level of theory and then the method. HF approach is usually available under *ab initio* level of theory while *density functional theory (DFT)* includes several HK alternatives, such as BP (implemented using [9] and [62]), BLYP (implemented using [9] and [52]) and B3LYP (implemented using [10] and [78]).

The choosing of a basis set is usually made between a series of alternatives including STO - Eq. (3.10), STO-G - Eq. (3.11) and its polarized [67] and diffuse [57] variants, GIAO [83], ANO [3], or others recently reviewed in [56], and refers mainly to the number of parameters involved in the characterization of an orbital function.

Our experience include the use of Spartan [44], HyperChem [46], Molecular Modeling Pro [12], ChemBioOffice [70], MPQC [70], and Gaussian [16].

Molecular geometry of the C_{32} ring (Fig. 2) was generated at DFT level of theory using BP ([9], [62]) method implemented in Spartan (for Spartan usage see [44]) with 6-311G* ([57]) basis set.

The manuals ([82] p. 494) suggest that 3-21G is sufficient for molecules consisting only of elements from the first two periods of the periodic system. However, considering the complexity of the studied assembly, 6-311G* ([67],[57]) basis set was chosen. BP represents one of the first approaches to solving equation 3.5 at the DFT level (in the formalism defined by 3.12).

In order to include the constraints related to symmetry in the model, the internal coordinate system was adopted and the geometry optimization was transferred to Gaussian (for Gaussian usage see [16]). Also an improved variant (B3LYP, [10], [78]) of BP was chosen (the B3LYP model being even more popular [60], and thus better documented). The optimization was done with B3LYP with 6-311G* as basis set.

Next step was to obtain the first member of the cluster family, cyclo[32]carbon[5]catenane. In order to accelerate the convergence, *ab-initio* HF ([29, 30, 25, 26]) STO-3G ([31]; convergence achieved in 54 steps), followed by 3-21G* ([57]; convergence achieved in 33 steps) and 6-31G* ([57]; convergence achieved in 10 steps) were used. A pattern of crossing has been identified and were further used to grow the cluster and the frame of the cluster generation was implemented.

Due to the simplicity in the representation of molecules, the HyperChem format (for HyperChem usage see [46]) was preferred for the generation of clusters starting from the C_{32} ring in Fig. 2.

4. RESULTS AND DISCUSSION

Gaussian software has been used to get symmetry constrained optimization (in Fig. 3) at B3LYP/6-311+G level of theory. Generated data is given in the Appendix A. The values of the parameters are extracted here:

$$a_0 = 1.2352 \text{ Å}; a_1 = 1.3356 \text{ Å} \tag{4.13}$$

Considering the typical lengths (p. 318 in [42]) of carbon-carbon single (1.531 Å), double (1.331 Å), and triple (1.205 Å) bonds one may regard the bonds associated with a_0 and a_1 bonds as being both double (but distinct one to the other) or the one with a_1 a single bond (with a strength comparable with a double bond) and the one with a_0 a triple bond (with a strength comparable with a double bond) (see Fig. 2).

Let be R the radius of the circumscribed circle of the C_{32} polyyne (see the C_{32} polyyne in Fig. 2). Using the notations from Fig. 3, the radius of the polyyne is the solution of the

Eq. (4.14) - see §4.1 in [44]:

$$\arcsin\frac{a_0}{2R} + \arcsin\frac{a_1}{2R} = \frac{2\pi}{n} \tag{4.14}$$

Using a_0 and a_1 from Eq. (4.13), the solution of Eq. (4.14) is given in Eq. (4.15).

$$R = 6.5557 \text{ Å} \tag{4.15}$$

A D_{16h} symmetry [59] for C_{32} represented in Fig. 2 is therefore established (Fig. 3, Eq. (4.13), Eq. (4.14), Eq. (4.15)).

The cluster of quadruple crossed cyclo[32]carbon[5]catenane has been build and is depicted in Fig. 4. The pattern identified in Fig. 4 is that all 4 rings intersect in perpendicular planes. Even more, the crossed section (z) is approximately of $R/2$ width ($z = 3.278$ Å $\approx R/2$, with R from Eq. (4.14)).

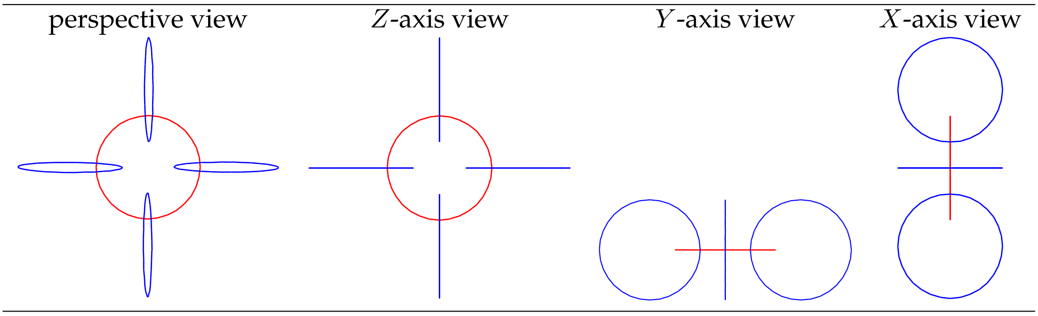

FIGURE 4. A cyclo[32]carbon[5]catenane (perspective view, and Z, Y and X axes projections)

The construction of the Fig. 4 cluster was thus achieved by copying, rotation from the horizontal plane to the vertical plane, the translation in the horizontal plane along the distance $R - z$, followed by the rotation with respect to an axis perpendicular to the horizontal plane in each instance by $\pi/2$ (Alg. 1).

Algorithm 1 Iterate C_{32} cluster

```
Input: $\tau, \Omega$    //current topology ($\tau$) and its outer rim ($\Omega$)
  //arrays containing coordinate versors (3), rotation versors (3), adjacencies (0-5)
  $ite_0 \leftarrow$ array(0,0,1, 0,0,0, 4,1,2,3,4)    //inner ring
  $ite_1 \leftarrow$ array(0,1,0, 1,0,0, 1,0)    //ring to the right
  $ite_2 \leftarrow$ array(0,1,0, -1,0,0, 1,0)    //ring to the left
  $ite_3 \leftarrow$ array(1,0,0, 0,1,0, 1,0)    //ring to the top
  $ite_4 \leftarrow$ array(1,0,0, 0,-1,0, 1,0)    //ring to the bottom
  for ( $i \leftarrow 0, \ldots,$ count($\Omega$)-1 )
    $k \leftarrow \Omega_i$; $m \leftarrow \tau_k$    //refer (as $m$) a outer rim ring
    rotate $\tau$ to get $m$ into (0,0,1) rotation position
    translate $\tau$ to get $m$ into (0,0,0) coordinate position
    for ( $j \leftarrow 2, \ldots, 4$ ) if $ite_j \notin \tau$ then $\tau \leftarrow \tau \cup ite_j$ endfor //add ite rings $\cap$ $m$ in $\tau$
    translate $\tau$ to get $m$ into its initial coordinate position
    rotate $\tau$ to get $m$ into its initial rotation position
  endfor
Output: $\tau$    //$\tau$ is the modified current topology
```

Alg. 1 applies the pattern from Fig. 4 to each outer rim rings and in one of its iterations add one more outer rim of rings to the current topology. In order that Alg. 1 to work in successions, after each iteration the list of outer rim rings must be updated.

Tab. 4 gives the information regarding the following congeners of the Fig. 4 cluster, which were obtained by the same procedure of copying, rotations and translations applied to each outer rim of the layer. For visibility, in Figs. 4 - 8 the colors of the rings were alternated (red and blue).

TABLE 4. Number of atoms in cyclo[32]carbon[n_l]catenanes by layers (l).

Fig.	Fig. 2	Fig. 4	Fig. 5	Fig. 6	Fig. 7	Fig. 8
l	0	1	2	3	4	5
n_l	1	5	17	45	95	171
Atoms	32	160	544	1440	3040	5472

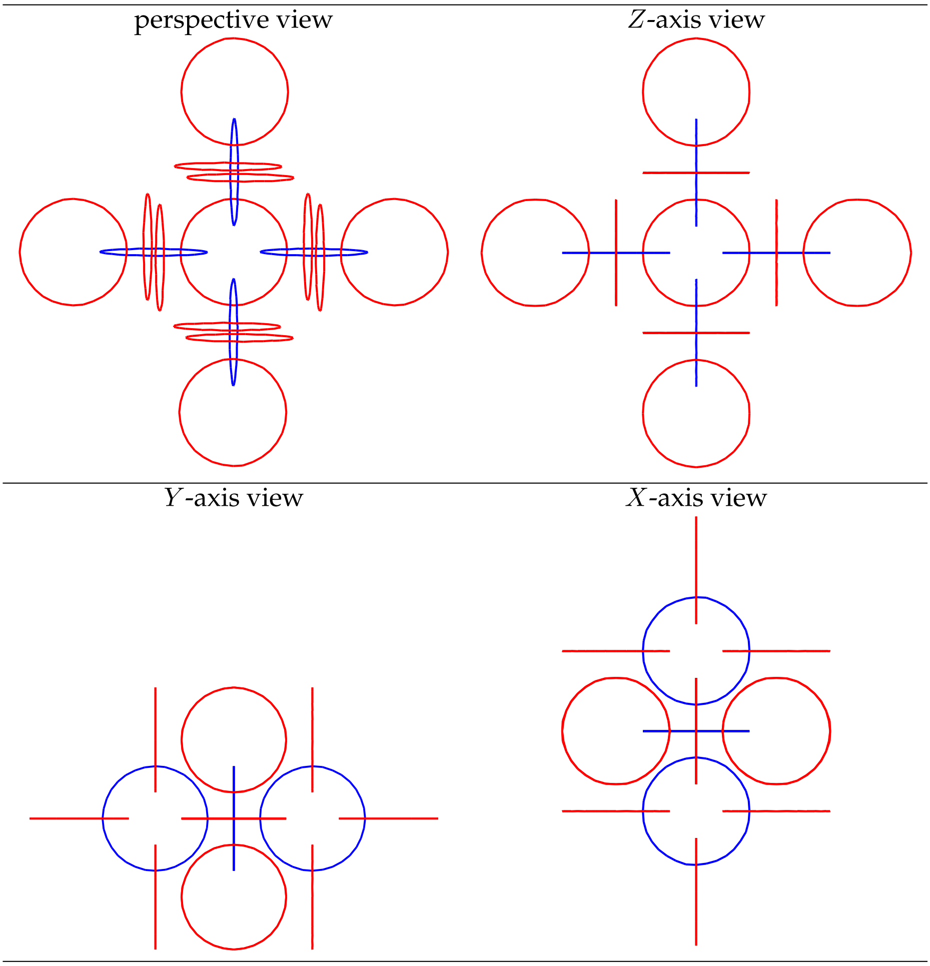
perspective view

Z-axis view

Y-axis view

X-axis view

FIGURE 5. A cyclo[32]carbon[17]catenane (perspective view, and Z, Y and X axes projections)

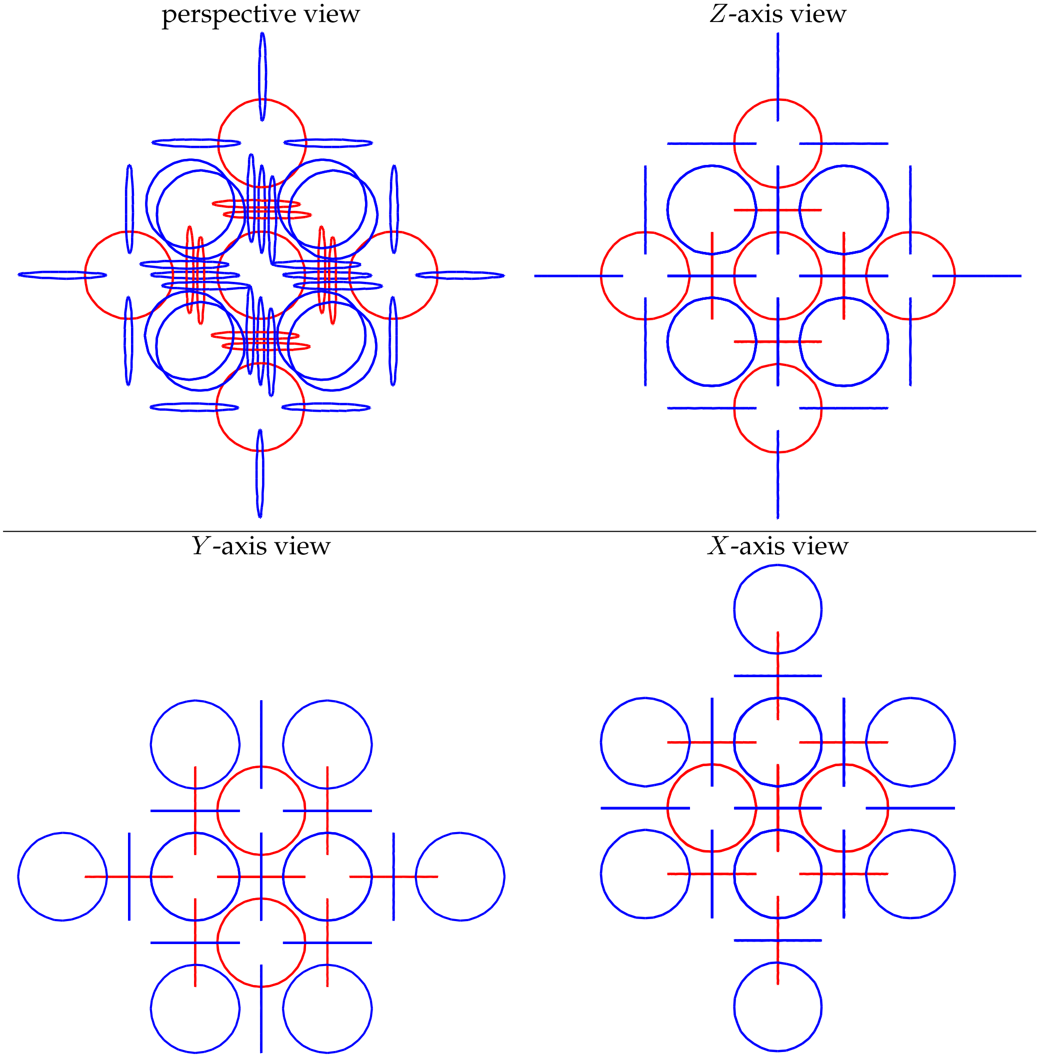
perspective view

Z-axis view

Y-axis view

X-axis view

FIGURE 6. A cyclo[32]carbon[45]catenane (perspective view, and Z, Y and X axes projections)

The series of n_l given in Tab. 4 is continued with $n_6 = 281$, $n_7 = 429$, $n_8 = 623$, $n_9 = 867$, $n_{10} = 1169$ (too big to be represented).

Based on the data from Tab. 4 the following recurrence relation has been established:

$$n_{l+4} - 5n_{l+3} + 9n_{l+2} + 7n_{l+1} + 2n_l = 0 \text{ for } l \geq 2 \tag{4.16}$$

It is expected that in the presence of other rings, the distances between atoms to suffer some minor changes and in the same time the whole structure to remain stable. A such stability study was conducted on cyclo[32]carbon[5]catenane (depicted in Fig. 4), which was small enough (160 heavy atoms, see entry 2 in Tab. 4) to address the symmetry constrained optimization at the same level of theory as for C_{32}. Appendix B contains the results of the optimization. Changes in the bond lengths are minor (a_0 from 1.2352 to 1.2569 Å, a_1 from 1.3356 to 1.3267 Å).

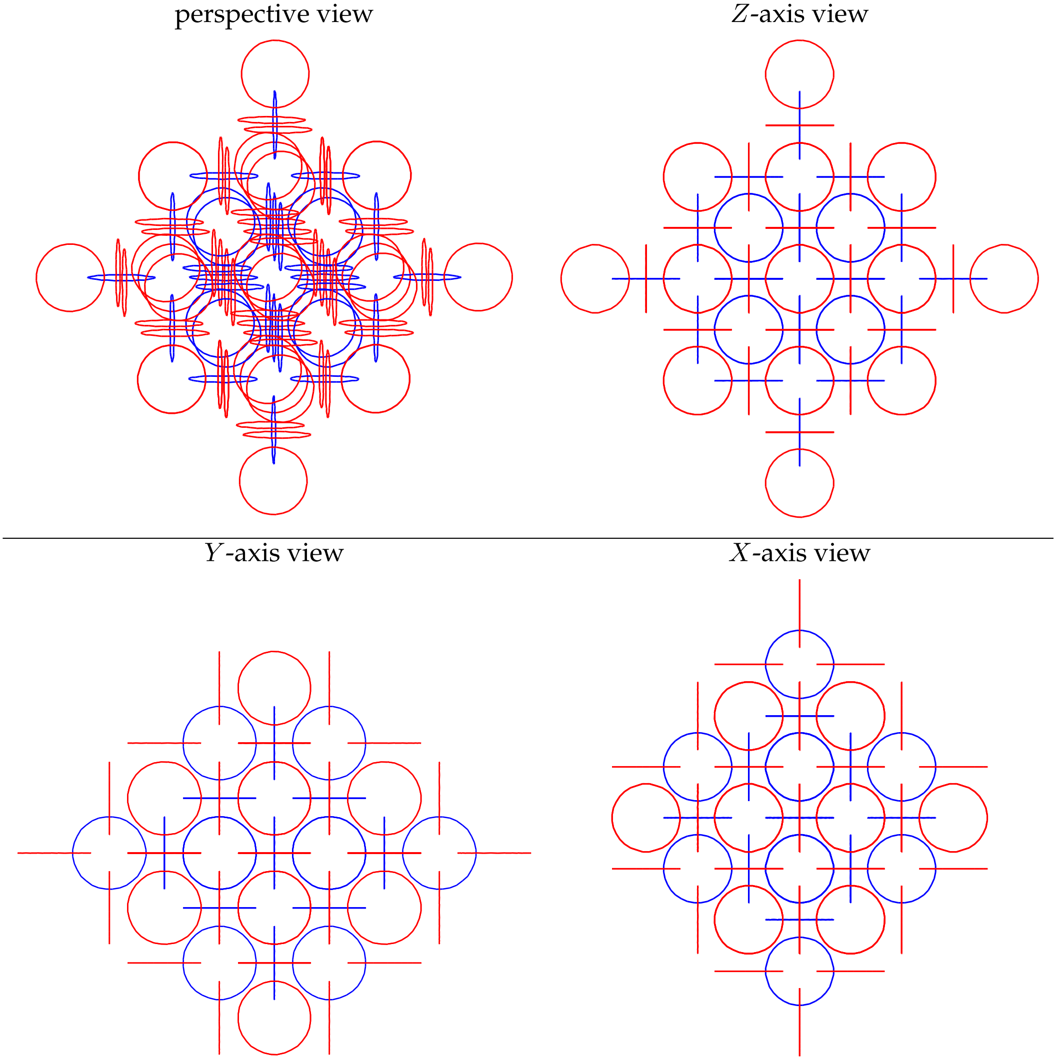

FIGURE 7. A cyclo[32]carbon[95]catenane (perspective view, and Z, Y and X axes projections)

Fig. 5 to Fig. 8 show the conformations of the first congeners of the series defined by Tab. 4. The alignment of the cluster with the coordinate system was done according to the axes of the main components of the eigenvalues according to the procedure described in [43].

In the Figs. 4 - 8 one can see the elegance of D_{4h} symmetry. Starting from $l = 2$ the shape of the ensemble approximates the largest part of an octahedron (Fig. 9).

The volume of bifrustum (Fig. 9), V_{sb}, is given by Eq. (4.17):

$$V_{sb} = \frac{h}{6} \frac{D^3 - d^3}{D - d} \tag{4.17}$$

where h is the height (between the two small bases) and d and D the diagonals of the squares of the bases.

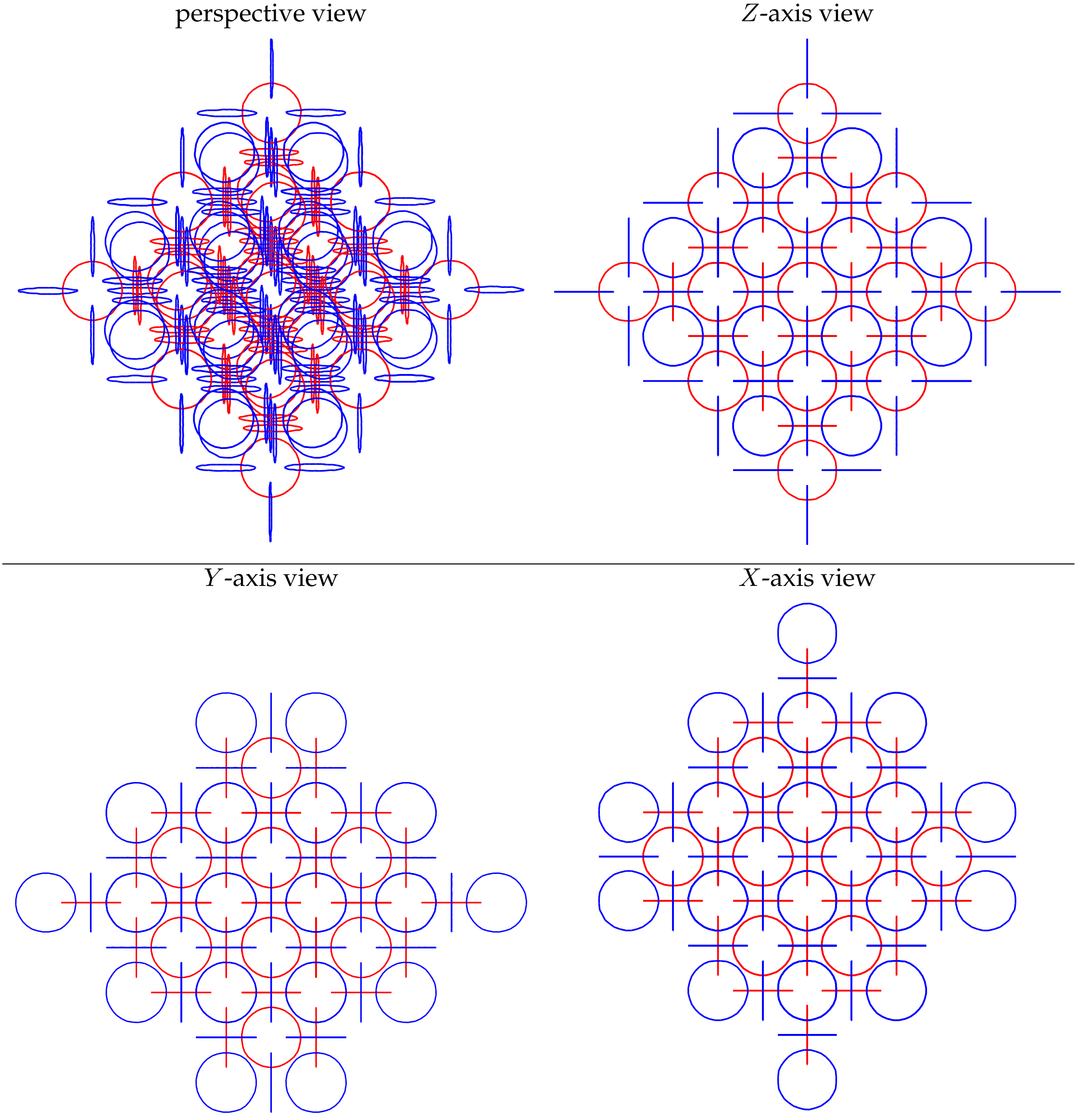
perspective view

Z-axis view

Y-axis view

X-axis view

FIGURE 8. A cyclo[32]carbon[171]catenane (perspective view, and Z, Y and X axes projections)

In order to proof the claim from Fig. 9, MatLab [58] software has been used to envelope the cyclo[32]carbon[$2 \cdot 3^l - 1$]catenanes ($l = 1, 2, ..., 8$) with more complex convex hulls [8]. The results regarding the approximated volume are given in Tab. 5.

In any instance the approximation of the constructed cyclo[32]carbon[n_l]catenanes with a bifrustum is remarkable with the increase of the cluster size. if at $l = 2$ the overlap is 93.05%, at $l = 8$ is 99.99%. One should notice that the arrangement constructed in this way seem not too compact, since a stack of rings located on the outside supports several crossings (Figs. 5 - 8).

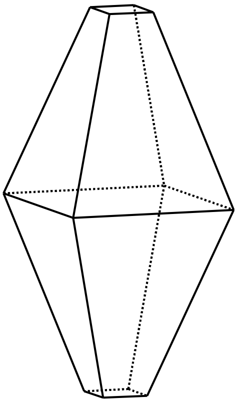

FIGURE 9. A square bifrustum approximating the convex hull of cyclo[32]carbon[$2 \cdot 3^l - 1$]catenane ($l = 2, 3, \ldots$)

TABLE 5. Approximating the volume of cyclo[32]carbon[n_l]catenanes

l	1	2	3	4	5	6	7	8
V_{ch}	5909	28320	73431	147448	260805	416857	628888	897403
V_{sb}	7044	30288	75508	150311	262305	419097	628293	897501
n_{ch}	124	188	124	188	124	188	124	188

V_{ch}: volume (in Å^3) with `convhulln` [8] MatLab [58] function; V_{sb}: volume (in Å^3) of bifrustum (Eq. (4.17), Fig. 9), $h = 3lR - R$, $d = 5R$, $D = 3lR + 2R$ (h is the height between the two small bases and d and D the diagonals of the squares of the bases); n_{ch}: number of `convhulln` vertices (the correspondent is always the same, $n_{sb} = 12$)

An alternate construction is obtained by iterating the catenating process by the three natural Cartesian coordinates (see for instance Z-axis view in Fig. 4). Fig. 10 shows a such arrangement.

It can be shown that if k even (such in Fig. 10, where $k = 6$) then k repetitions in each direction produces a total number of $\frac{3}{4}k^3$ rings (162 rings in Fig. 10) that are contained in a cube of size $\frac{3k+1}{2}R$ (a size of $9.5R$ in Fig. 10). The density then is:

$$\rho_k = \frac{256 \cdot 10^4}{18.069 \cdot R} \frac{n^3}{(n+1/3)^3} \text{ kg/m}^3, \text{ for } k \text{ even} \tag{4.18}$$

with a limit value $\rho_\infty = 502.56$ kg/m^3 (R is the one provided by Eq. (4.14)).

A similar calculation for the bifrustum arrangement (Figs. 5 - 8) gives 383 kg/m^3, 391 kg/m^3, 411 kg/m^3, and 418 kg/m^3, for Fig. 5, Fig. 6, Fig. 7 and Fig. 8 catenanes respectively.

Symmetry constrained model of C_{32} cyclic polyyne from Fig. 3 has been used intensively in this paper. According to this model, to characterize the cyclic polyyne only two parameters are needed (are to be determined): the length of the triple bond (a_0 in Fig. 3, obtained for the even indices feed into s function) and the length of the single bond (a_1 in Fig. 3, obtained for the odd indices feed into s function). These two parameters uniquely determine the R value (polyyne ring radius, Eq. (4.14)). Polyyne cluster has been further obtained by simple translations and rotations of the polyyne molecule. Note that from the chemical point of view the formation of a catenane requires breaking and bonding again of the ring or bending of the linear polyyne and formation of the ring on site. The use

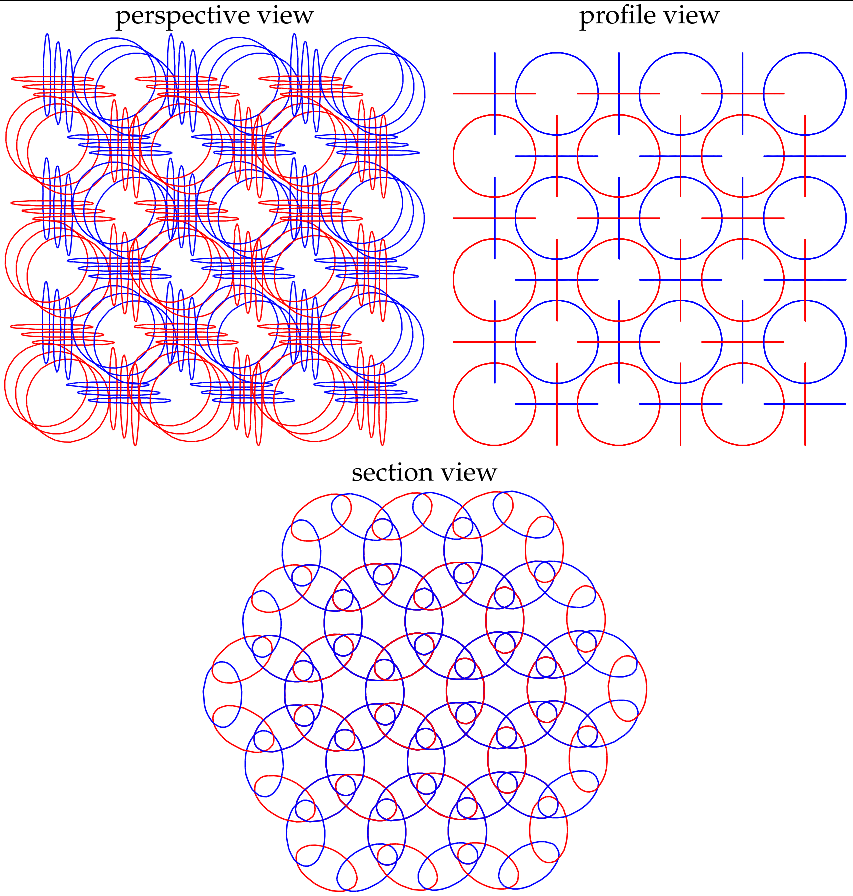

FIGURE 10. A cyclo[32]carbon[162]catenane (6 chained rings in each orthogonal direction)

of internal coordinates combined with symmetry constrains simplifies a lot the molecule specification. For the polyyne cluster along with the two aforementioned parameters (a_0 and a_1, Eq. (4.17)), are necessary only a translation parameter (noted with z and identified in the case of C_{32} crosses - see Fig. 4 - as being half of the radius R) and some constant rotation parameters to change the alignment of the polyyne from xy plane into xz and yz planes. Advantages other than simplification of the problem for the use of internal coordinates system has been reported elsewhere [5].

Due to the complexity of the system, the level of refinement is relatively low. Therefore, one may question the level of theory used to do the computations. For instance, recent variations of the classical methods has been reported: CAM-B3LYP in [84], ωB97 in [17], LC-ωHPBE in [32], APF in [4]. In the defense of methods used (HF, BP and B3LYP) may stay the fact that actually the improvement reported in the context of the use of the new methods is in the presence of heteroatoms (N, O, S, P instead of C; for CAM-B3LYP reported in [84]), non-covalent interactions (ωB97X-D and its relatives, ωB97 and ωB97X reported in [17]), for diatomic molecules of different elements and dimers of small hydrocarbons [4], and finally reaction barrier heights and Rydberg excitation energies of heteroatomic molecules for LC-ωHPBE [32], none of them being the case here.

The identified bifrustum geometry (Fig. 9, of D_{4h} symmetry) for the layer-based arrangement (cluster growth in Figs 5 - 8) approaches, in convergence ($l \to \infty$), the octahedral (O_h) arrangement ($D = 3lR+2R$; $h = 3lR-R$; $D \approx h$ for large l), and in this instance it is only a matter of threshold [64] to distinguish between the two.

From hexavalent atoms, Ruthenium [49] and Uranium [80] is known to adopt O_h and D_{4h} conformations, while tetravalent includes Titanium [1] and Vanadium [27]. Evan if appears more often for planar compounds, D_{4h} point group is one of the most common molecular symmetries found in nature. Porphyrin complexes consist of a square planar core [54].

Tetravalent compounds (such as of Copper and Nickel reported in [71]) are the topological relatives of the bifrustum conformation.

The energy of the system provides important information about the role of clustering in the stabilization of the C_{32} rings. It was shown that a series of important molecular parameters (nodal structure, order of the energy levels, prediction of molecular shape, and changes in hybridization and ionization potential with angle [2]) are reflected in the extended Hückel energy ([33]), the calculated values of Slater based [73] single point extended Hückel energy given in Tab. 6 (in Hartree, 1 Hartree ≈ 72395 J/mol)) were used to make qualitative judgments about the stabilization by clustering.

TABLE 6. Binding energy of several cyclo[32]carbon[n]catenanes

$-E$	x_0	x_1	x_2	x_3	x_4	**Representation**
52639	1	0	0	0	0	Fig. 2
263183	5	4	0	0	1	Fig. 4
315815	6	0	6	0	0	Fig. 10 with 2 instead of 6 (and 6 instead of 162)
684270	13	8	0	4	1	Fig. 5 with 4 (Z-axis view) outer rims removed
894813	17	12	0	0	5	Fig. 5
1052706	20	0	12	8	0	Fig. 10 with 3 instead of 6 and central rim removed
1105333	21	0	8	12	1	Fig. 10 with 2 instead of 6 (and 6 instead of 162)
1894845	36	0	11	18	7	Fig. 10 with 3 × 4 instead of 6×6
2520724	48	0	12	24	12	Fig. 10 with 4 instead of 6 (and 48 instead of 162)

$\boldsymbol{E}$: extended Hückel energy (rounded values from HyperChem software
$\boldsymbol{x_0}$: number of C_{32} rings ($32 \cdot \boldsymbol{x_0}$ is the number of Carbon atoms)
$\boldsymbol{x_1}$: number of C_{32} rings crossed by (only) one (another) C_{32} ring
$\boldsymbol{x_2}$: number of C_{32} rings crossed by two C_{32} rings
$\boldsymbol{x_3}$: number of rings crossed by three rings; $\boldsymbol{x_4}$: number of rings crossed by four rings

A linear regression (with no intercept) with data from Tab. 6 is significant (Eq. (4.19)).

$$E \sim \hat{E} = -52638.896_{\pm 0.01} x_0 + 1.495_{\pm 0.004} \sum_{i=1}^{4} i \cdot x_i \tag{4.19}$$

where the variables E and x_i with the meaning and the values from Tab. 6.

The equation (4.19) shows that almost entirely the energy of the cluster is given by its rings and only a very small amount of the contribution (less than 0.003%) is given by its crosses. The coefficient of x_i for $i = 1, 2, 3, 4$ is positive, so it is an very small (less than 0.003%) energetical cost with each cross.

Both discussed arrangements - bifstrum like (Figures 5 - 8) and Cartesian directions iterated net (Fig. 10) are highly symmetrical. In fact, both express actually one and the same crystalline net. Let us imagine that in Fig. 10 a red circle is a Natrium atom, and a blue circle is a Chlorine atom. It became obvious that the net is a (little more complex) face-centered cubic lattice. Regarding the second statement, that the bifstrum like arrangement is the same net, it is enough to say that both arrangements are obtained by the same symmetry operations (same rotations and translations of the C_{32} ring) and the results are placed in same relative position, and each neighboring ring of a ring in same relative position in both instances.

The large number of atoms did not allow the study to be carried out at a high level of theory and with a basis function too large than in the case of the C_{32} ring. The use of symmetry (see Fig. 3), however, dramatically reduces the complexity of the problem. The catenane networks proposed by the chaining of C_{32} have a very good geometric arrangement (face centered cubic) and present a special potential for exploitation through the prism of its expected properties.

5. Conclusions

This study has shown that by crossing C_{32} cyclic polyynes if succeeded is obtained a material about four times lighter than graphite (and with half the density of water, see Eq. 4.18) but with a hardness comparable to that of diamond (due to the alternation of simple and triple bonds) and with incredible elasticity due to the catenation (chained shape of the molecules).

Acknowledgments

The authors are grateful for all comments from reviewers and editors regarding the improvement of the final version of the manuscript.

Appendix A. Gaussian B3LYP 6-311+G optimization output for C_{32}

```
1|1|UNPC-DESKTOP-F4T462M|FOpt|RB3LYP|6-311+G|C32|DESKTOP|27-May-2023|1
||#B3LYP/6-311+G opt=(Z-matrix,maxcycle=1000)||C32 polyyne optimizatio
n||0,1|C|C,1,b1|C,2,b3,1,a0|C,3,b1,2,a0,1,d0,0|C,4,b3,3,a0,2,d0,0|C,5,
b1,4,a0,3,d0,0|C,6,b3,5,a0,4,d0,0|C,7,b1,6,a0,5,d0,0|C,8,b3,7,a0,6,d0,
0|C,9,b1,8,a0,7,d0,0|C,10,b3,9,a0,8,d0,0|C,11,b1,10,a0,9,d0,0|C,12,b3,
11,a0,10,d0,0|C,13,b1,12,a0,11,d0,0|C,14,b3,13,a0,12,d0,0|C,15,b1,14,a
0,13,d0,0|C,16,b3,15,a0,14,d0,0|C,17,b1,16,a0,15,d0,0|C,18,b3,17,a0,16
,d0,0|C,19,b1,18,a0,17,d0,0|C,20,b3,19,a0,18,d0,0|C,21,b1,20,a0,19,d0,
0|C,22,b3,21,a0,20,d0,0|C,23,b1,22,a0,21,d0,0|C,24,b3,23,a0,22,d0,0|C,
25,b1,24,a0,23,d0,0|C,26,b3,25,a0,24,d0,0|C,27,b1,26,a0,25,d0,0|C,28,b
3,27,a0,26,d0,0|C,29,b1,28,a0,27,d0,0|C,30,b3,29,a0,28,d0,0|C,31,b1,30
,a0,29,d0,0||b3=1.23515276|b1=1.33561459|a0=168.75|d0=0.||Version=IA32
W-G09RevD.01|HF=-1218.5487807|RMSD=9.857e-009|RMSF=1.490e-006|Dipole=0
.,0.,0.|Quadrupole=-0.9486494,1.8972987,-0.9486494,0.,0.,0.|PG=D16H [S
GH(C32)]||@
```

Appendix B. Gaussian B3LYP 6-311+G optimization output for $5C_{32}$

```
1|1|UNPC-DESKTOP-F4T462M|FOpt|RB3LYP|6-311+G|5C32|DESKTOP|30-June-2023
|1||#B3LYP/6-311+G opt=(Z-matrix)||second step - the 5C32 polyyne clus
ter optimization||0,1\C\C,1,c2\C,2,c3,1,c1\C,3,c2,2,c1,1,c0,0\C,4,c3,3
,c1,2,c0,0\C,5,c2,4,c1,3,c0,0\C,6,c3,5,c1,4,c0,0\C,7,c2,6,c1,5,c0,0\C,
8,c3,7,c1,6,c0,0\C,9,c2,8,c1,7,c0,0\C,10,c3,9,c1,8,c0,0\C,11,c2,10,c1,
9,c0,0\C,12,c3,11,c1,10,c0,0\C,13,c2,12,c1,11,c0,0\C,14,c3,13,c1,12,c0
,0\C,15,c2,14,c1,13,c0,0\C,16,c3,15,c1,14,c0,0\C,17,c2,16,c1,15,c0,0\C
,18,c3,17,c1,16,c0,0\C,19,c2,18,c1,17,c0,0\C,20,c3,19,c1,18,c0,0\C,21,
c2,20,c1,19,c0,0\C,22,c3,21,c1,20,c0,0\C,23,c2,22,c1,21,c0,0\C,24,c3,2
3,c1,22,c0,0\C,25,c2,24,c1,23,c0,0\C,26,c3,25,c1,24,c0,0\C,27,c2,26,c1
,25,c0,0\C,28,c3,27,c1,26,c0,0\C,29,c2,28,c1,27,c0,0\C,30,c3,29,c1,28,
c0,0\C,1,c3,2,c9,3,c0,0\C,25,c6,24,c10,23,c22,0\C,33,c2,25,c11,24,c23,
```

```
0\C,34,c3,33,c1,25,c0,0\C,35,c2,34,c1,33,c0,0\C,36,c3,35,c1,34,c0,0\C,
37,c2,36,c1,35,c0,0\C,38,c3,37,c1,36,c0,0\C,39,c2,38,c1,37,c0,0\C,40,c
3,39,c1,38,c0,0\C,41,c2,40,c1,39,c0,0\C,42,c3,41,c1,40,c0,0\C,43,c2,42
,c1,41,c0,0\C,44,c3,43,c1,42,c0,0\C,45,c2,44,c1,43,c0,0\C,46,c3,45,c1,
44,c0,0\C,47,c2,46,c1,45,c0,0\C,48,c3,47,c1,46,c0,0\C,49,c2,48,c1,47,c
0,0\C,50,c3,49,c1,48,c0,0\C,51,c2,50,c1,49,c0,0\C,52,c3,51,c1,50,c0,0\
C,53,c2,52,c1,51,c0,0\C,54,c3,53,c1,52,c0,0\C,55,c2,54,c1,53,c0,0\C,56
,c3,55,c1,54,c0,0\C,57,c2,56,c1,55,c0,0\C,58,c3,57,c1,56,c0,0\C,59,c2,
58,c1,57,c0,0\C,60,c3,59,c1,58,c0,0\C,61,c2,60,c1,59,c0,0\C,62,c3,61,c
1,60,c0,0\C,33,c3,25,c12,24,c24,0\C,1,c7,2,c13,3,c25,0\C,65,c2,1,c14,2
,c26,0\C,66,c3,65,c1,1,c0,0\C,67,c2,66,c1,65,c0,0\C,68,c3,67,c1,66,c0,
0\C,69,c2,68,c1,67,c0,0\C,70,c3,69,c1,68,c0,0\C,71,c2,70,c1,69,c0,0\C,
72,c3,71,c1,70,c0,0\C,73,c2,72,c1,71,c0,0\C,74,c3,73,c1,72,c0,0\C,75,c
2,74,c1,73,c0,0\C,76,c3,75,c1,74,c0,0\C,77,c2,76,c1,75,c0,0\C,78,c3,77
,c1,76,c0,0\C,79,c2,78,c1,77,c0,0\C,80,c3,79,c1,78,c0,0\C,81,c2,80,c1,
79,c0,0\C,82,c3,81,c1,80,c0,0\C,83,c2,82,c1,81,c0,0\C,84,c3,83,c1,82,c
0,0\C,85,c2,84,c1,83,c0,0\C,86,c3,85,c1,84,c0,0\C,87,c2,86,c1,85,c0,0\
C,88,c3,87,c1,86,c0,0\C,89,c2,88,c1,87,c0,0\C,90,c3,89,c1,88,c0,0\C,91
,c2,90,c1,89,c0,0\C,92,c3,91,c1,90,c0,0\C,93,c2,92,c1,91,c0,0\C,94,c3,
93,c1,92,c0,0\C,65,c3,1,c15,2,c27,0\C,17,c4,16,c16,15,c28,0\C,97,c2,17
,c17,16,c29,0\C,98,c3,97,c1,17,c0,0\C,99,c2,98,c1,97,c0,0\C,100,c3,99,
c1,98,c0,0\C,101,c2,100,c1,99,c0,0\C,102,c3,101,c1,100,c0,0\C,103,c2,1
02,c1,101,c0,0\C,104,c3,103,c1,102,c0,0\C,105,c2,104,c1,103,c0,0\C,106
,c3,105,c1,104,c0,0\C,107,c2,106,c1,105,c0,0\C,108,c3,107,c1,106,c0,0\
C,109,c2,108,c1,107,c0,0\C,110,c3,109,c1,108,c0,0\C,111,c2,110,c1,109,
c0,0\C,112,c3,111,c1,110,c0,0\C,113,c2,112,c1,111,c0,0\C,114,c3,113,c1
,112,c0,0\C,115,c2,114,c1,113,c0,0\C,116,c3,115,c1,114,c0,0\C,117,c2,1
16,c1,115,c0,0\C,118,c3,117,c1,116,c0,0\C,119,c2,118,c1,117,c0,0\C,120
,c3,119,c1,118,c0,0\C,121,c2,120,c1,119,c0,0\C,122,c3,121,c1,120,c0,0\
C,123,c2,122,c1,121,c0,0\C,124,c3,123,c1,122,c0,0\C,125,c2,124,c1,123,
c0,0\C,126,c3,125,c1,124,c0,0\C,97,c3,17,c18,16,c30,0\C,9,c5,8,c19,7,c
31,0\C,129,c2,9,c20,8,c32,0\C,130,c3,129,c1,9,c0,0\C,131,c2,130,c1,129
,c0,0\C,132,c3,131,c1,130,c0,0\C,133,c2,132,c1,131,c0,0\C,134,c3,133,c
1,132,c0,0\C,135,c2,134,c1,133,c0,0\C,136,c3,135,c1,134,c0,0\C,137,c2,
136,c1,135,c0,0\C,138,c3,137,c1,136,c0,0\C,139,c2,138,c1,137,c0,0\C,14
0,c3,139,c1,138,c0,0\C,141,c2,140,c1,139,c0,0\C,142,c3,141,c1,140,c0,0
\C,143,c2,142,c1,141,c0,0\C,144,c3,143,c1,142,c0,0\C,145,c2,144,c1,143
,c0,0\C,146,c3,145,c1,144,c0,0\C,147,c2,146,c1,145,c0,0\C,148,c3,147,c
1,146,c0,0\C,149,c2,148,c1,147,c0,0\C,150,c3,149,c1,148,c0,0\C,151,c2,
150,c1,149,c0,0\C,152,c3,151,c1,150,c0,0\C,153,c2,152,c1,151,c0,0\C,15
4,c3,153,c1,152,c0,0\C,155,c2,154,c1,153,c0,0\C,156,c3,155,c1,154,c0,0
\C,157,c2,156,c1,155,c0,0\C,158,c3,157,c1,156,c0,0\C,129,c3,9,c21,8,c3
3,0\\c2=1.32667598\c3=1.25685912\c4=4.02743752\c5=6.74877158\c6=8.0996
1993\c7=9.26287576\c9=168.77982421\c10=91.85676211\c11=66.98305268\c12
=101.76206714\c13=97.70982214\c14=83.598515\c15=85.14256563\c16=86.732
87207\c17=75.91782528\c18=92.81859516\c19=90.95260341\c20=107.35926725
\c21=61.37341641\c22=227.81743274\c23=86.97387078\c24=266.97127511\c25
=181.95830982\c26=89.67126798\c27=269.66938991\c28=337.35232344\c29=88
.34910889\c30=268.34888019\c31=255.77391797\c32=266.36446291\c33=86.36
329052\c0=0.\c1=168.75\\Version=ES64L-G16RevA.03\State=1-A\HF=-6092.98
17907\RMSD=5.898e-09\RMSF=4.802e-05\Dipole=-0.0004099,-0.0002089,0.000
059\Quadrupole=-0.1287811,0.3107265,-0.1819454,0.0045478,0.0047578,-0.
0089417\PG=C01 [X(C160)]\\@
```

References

[1] Ahuja H., Jain S., and Rivest R., Co-ordination complexes of titanium(IV) halides. preparation and infra-red spectra of the complexes of titanium(iv) halides with cyclic thioethers, *J. Inorg. Nucl. Chem.* **30** (1968), no. 9, 2459–2466. URL `http://sciencedirect.com/science/article/pii/0022190268802581`.

[2] Allen L. C. and Russell J. D., Extended Hückel theory and the shape of molecules, *J. Chem. Phys.* **46** (1967), no. 3, 1029–1037. URL `http://doi.org/10.1063/1.1840764`.

[3] Almlöf J. and Taylor P. R., General contraction of gaussian basis sets. I. Atomic natural orbitals for first- and second-row atoms, *J.Chem. Phys.* **86** (1987), no. 7, 4070–4077. URL `http://doi.org/10.1063/1.451917`.

[4] Austin A. et al., A density functional with spherical atom dispersion terms, *J. Chem. Theory Comput.* **8** (2012), no. 12, 4989–5007. URL `http://doi.org/10.1021/ct300778e`.

[5] Baker J., Techniques for geometry optimization: A comparison of cartesian and natural internal coordinates, *J. Comput. Chem.* **14** (1993), no. 9, 1085–1100. URL `http://onlinelibrary.wiley.com/doi/abs/10.1002/jcc.540140910`.

[6] Baker J., Kessi A., and Delley B., The generation and use of delocalized internal coordinates in geometry optimization, *J. Chem. Phys.* **105** (1996), no. 1, 192–212. URL `http://doi.org/10.1063/1.471864`.

[7] Balàzs N. L., Formation of stable molecules within the statistical theory of atoms, *Phys. Rev.* **156** (1967), 42–47. URL `http://link.aps.org/doi/10.1103/PhysRev.156.42`.

[8] Barber C. B., Dobkin D. P., and Huhdanpaa H., The quickhull algorithm for convex hulls, *ACM Trans. Math. Softw.* **22** (1996), no. 4, 469–483. URL `http://doi.org/10.1145/235815.235821`.

[9] Becke A. D., Density-functional exchange-energy approximation with correct asymptotic behavior, *Phys. Rev. A* **38** (1988), 3098–3100. URL `https://link.aps.org/doi/10.1103/PhysRevA.38.3098`.

[10] Becke A. D., Density-functional thermochemistry. III. The role of exact exchange, *The Journal of Chemical Physics* **98** (1993), no. 7, 5648–5652. URL `http://doi.org/10.1063/1.464913`.

[11] Bohr N., Can quantum-mechanical description of physical reality be considered complete?, *Phys. Rev.* **48** (1935), 696–702. URL `http://link.aps.org/doi/10.1103/PhysRev.48.696`.

[12] Bolboacă S. D. et al., Molecular descriptors family on vertex cutting: Relationships between acelazolamide structures and their inhibitory activity, *Appl. Med. Inform.* **25** (2011), no. 3, 4, 65–74. URL `http://ami.info.umfcluj.ro/index.php/AMI/article/view/94`.

[13] Born M. and Oppenheimer R., Zur quantentheorie der molekeln, *Ann. Phys.* **389** (1927), no. 20, 457–484. URL `http://onlinelibrary.wiley.com/doi/abs/10.1002/andp.19273892002`.

[14] Bryce M. R., A review of functional linear carbon chains (oligoynes, polyynes, cumulenes) and their applications as molecular wires in molecular electronics and optoelectronics, *J. Mater. Chem. C* **9** (2021), 10524–10546. URL `http://dx.doi.org/10.1039/D1TC01406D`.

[15] Brémond E. et al., Stability of the polyynic form of C_{18}, C_{22}, C_{26}, and C_{30} nanorings: a challenge tackled by range-separated double-hybrid density functionals, *Phys. Chem. Chem. Phys.* **24** (2022), 4515–4525. URL `http://doi.org/10.1039/D1CP04996H`.

[16] Bálint D. and Jäntschi L., Comparison of molecular geometry optimization methods based on molecular descriptors, *Mathematics* **9** (2021), no. 22, 2855. URL `http://dx.doi.org/10.3390/math9222855`.

[17] Chai J.-D. and Head-Gordon M., Long-range corrected hybrid density functionals with damped atom–atom dispersion corrections, *Phys. Chem. Chem. Phys.* **10** (2008), 6615–6620. URL `http://doi.org/10.1039/B810189B`.

[18] Chalifoux W. A. and Tykwinski R. R., Synthesis of polyynes to model the sp-carbon allotrope carbyne, *Nat. Chem.* **2** (2010), no. 11, 967–971. URL `http://doi.org/10.1038/nchem.828`.

[19] Dietrich-Buchecker C. O. et al., High-yield synthesis of a dicopper(I) trefoil knot containing 1,3-phenylene groups as bridges between the chelate units, *J. Chem. Soc. Chem. Commun.* **0** (1994), 2231–2232. URL `http://doi.org/10.1039/C39940002231`.

[20] Diudea M. V., Gutman I., and Jäntschi L., *Molecular Topology*, Nova Science Publishers, Huntington, N.Y., 2001. URL `http://lccn.loc.gov/2001031282`.

[21] Doverstål M. et al., Carbon cluster studies, *Phys. Scr.* **43** (1991), no. 6, 572. URL `http://doi.org/10.1088/0031-8949/43/6/006`.

[22] Einstein A., Podolsky B., and Rosen N., Can quantum-mechanical description of physical reality be considered complete?, *Phys. Rev.* **47** (1935), 777–780. URL `https://link.aps.org/doi/10.1103/PhysRev.47.777`.

[23] Euler L., Elementa doctrinae solidorum, *Novi Comment. Acad. Sci. Imp. Petropol.* **4** (1758), 109–140. URL `http://biodiversitylibrary.org/item/125754`.

[24] Feyereisen M. et al., Relative stabilities of fullerene, cumulene, and polyacetylene structures for C_n: n=18-60, *J. Chem. Phys.* **96** (1992), 2926–2932. URL `http://doi.org/10.1063/1.461989`.

[25] Fock V., Näherungsmethode zur lösung des quantenmechanischen mehrkörperproblems, *Z. Phys.* **61** (1930), no. 1, 126–148. URL `http://doi.org/10.1007/BF01340294`.

[26] Fock V., "Selfconsistent field" mit austausch für natrium, *Z. Phys.* **62** (1930), no. 11, 795–805. URL `http://doi.org/10.1007/BF01330439`.

[27] Gloter A. et al., Vanadium valency and hybridization in V-doped hafnia investigated by electron energy loss spectroscopy, *Eur. Phys. J. B* **22** (2001), no. 2, 179–186. URL `http://doi.org/10.1007/PL00011142`.

[28] Grutter M. et al., Electronic absorption spectra of the polyacetylene chains $HC_{2n}H$, $HC_{2n}H^-$, and $HC_{2n-1}N^-$ ($n = 6 - 12$) in neon matrixes, *J. Phys. Chem. A* **102** (1998), no. 48, 9785–9790. URL `http://doi.org/10.1021/jp983185t`.

[29] Hartree D. R., The wave mechanics of an atom with a non-coulomb central field. Part I. Theory and methods, *Math. Proc. Cambridge Phil. Soc.* **24** (1928), no. 1, 89–110.

[30] Hartree D. R., The wave mechanics of an atom with a non-coulomb central field. Part II. Some results and discussion, *Math. Proc. Cambridge Phil. Soc.* **24** (1928), no. 1, 111–132.

[31] Hehre W. J., Stewart R. F., and Pople J. A., Self-consistent molecular-orbital methods. I. Use of gaussian expansions of slater-type atomic orbitals, *J. Chem. Phys.* **51** (1969), no. 6, 2657–2664. URL `https://doi.org/10.1063/1.1672392`.

[32] Henderson T. M. et al., Can short-range hybrids describe long-range-dependent properties?, *The Journal of Chemical Physics* **131** (2009), no. 4, 044108. URL `http://doi.org/10.1063/1.3185673`, 044108.

[33] Hoffmann R., An extended Hückel theory. I. Hydrocarbons, *J. Chem. Phys.* **39** (1963), no. 6, 1397–1412. URL `http://doi.org/10.1063/1.1734456`.

[34] Hohenberg P. and Kohn W., Inhomogeneous electron gas, *Phys. Rev.* **136** (1964), B864–B871. URL `http://link.aps.org/doi/10.1103/PhysRev.136.B864`.

[35] Hu Y. et al., Kohn-sham density functional theory of abelian anyons, *Phys. Rev. B* **103** (2021), 035124. URL `http://link.aps.org/doi/10.1103/PhysRevB.103.035124`.

[36] Hunter J., Fye J., and Jarrold M. F., Annealing C_{60}^+: Synthesis of fullerenes and large carbon rings, *Science* **260** (1993), no. 5109, 784–786. URL `http://science.org/doi/abs/10.1126/science.260.5109.784`.

[37] Hutter J., Luethi H. P., and Diederich F., Structures and vibrational frequencies of the carbon molecules C_2-C_{18} calculated by density functional theory, *J. Am. Chem. Soc.* **116** (1994), no. 2, 750–756. URL `http://doi.org/10.1021/ja00081a041`.

[38] Iqbal Z. et al., Evidence for a solid phase of dodecahedral C_{20}, *Eur. Phys. J. B* **31** (2003), no. 4, 509–515. URL `https://doi.org/10.1140/epjb/e2003-00060-4`.

[39] Jäntschi L., Bolboacă S. D., and Janežic D., Cyclic carbon polyynes, *Carbon Mater. Chem. Phys.* **9** (2016), 423–436. URL `http://doi.org/10.1007/978-3-319-31584-3_23`.

[40] Januszewski J. A. and Tykwinski R. R., Synthesis and properties of long $[n]$cumulenes ($n \geq 5$), *Chem. Soc. Rev.* **43** (2014), 3184–3203. URL `http://doi.org/10.1039/C4CS00022F`.

[41] Jones R. O., Density functional study of carbon clusters C_{2n} ($2 \leq n \leq 16$). i. structure and bonding in the neutral clusters, *J. Chem. Phys.* **110** (1999), no. 11, 5189–5200. URL `http://doi.org/10.1063/1.478414`.

[42] Jäntschi L., *General Chemistry*, 3rd edn., AcademicDirect, Cluj-Napoca, Romania, 2013. URL: `http://ph.academicdirect.org/GCC_v3.pdf`.

[43] Jäntschi L., The eigenproblem translated for alignment of molecules, *Symmetry* **11** (2019), no. 8, 1027. URL `http://dx.doi.org/10.3390/sym11081027`.

[44] Jäntschi L., Energetics of $C_8B_8N_8$, $N_{12}B_{12}$, and C_{24} macrocycles and two [4]catenanes, *Foundations* **2** (2022), no. 3, 781–797. URL `http://doi.org/10.3390/foundations2030053`.

[45] Jäntschi L., Triple crossed 3 C_{26} cyclic cumulene catenane, *Fullerenes, Nanotubes and Carbon Nanostructures* **0** (2024), no. 0, 1–15. URL `http://doi.org/10.1080/1536383X.2024.2354721`.

[46] Jäntschi L. and Bolboacă S. D., Conformational study of C_{24} cyclic polyyne clusters, *Int. J. Quantum Chem.* **118** (2018), no. 15, e25614. URL `http://onlinelibrary.wiley.com/doi/abs/10.1002/qua.25614`.

[47] Kekulé A., Ueber die s. g. gepaarten verbindungen und die theorie der mehratomigen radicale, *Justus Liebigs Ann. Chem.* **104** (1857), no. 2, 129–150. URL `http://chemistry-europe.onlinelibrary.wiley.com/doi/abs/10.1002/jlac.18571040202`.

[48] Kekulé A., Ueber die constitution und die metamorphosen der chemischen verbindungen und über die chemische natur des kohlenstoffs, *Justus Liebigs Ann. Chem.* **106** (1858), no. 2, 129–159. URL `http://chemistry-europe.onlinelibrary.wiley.com/doi/abs/10.1002/jlac.18581060202`.

[49] Kimura T. et al., Preparation and characterization of nonclassical tetraazaporphyrin, bis(4-methylpyridine)[1,3,5,7,9,11,13,15-octaphenyltetra(3,4-thieno)tetraazaporphyrinato]ruthenium(ii), *Eur. J. Inorg. Chem.* **2011** (2011), no. 6, 888–894. URL `http://chemistry-europe.onlinelibrary.wiley.com/doi/abs/10.1002/ejic.201001094`.

[50] Kloster-Jensen E., Haink H.-J., and Christen H., The electronic spectra of unsubstituted mono- to pentaacetylene in the gas phase and in solution in the range 1100 to 4000 Å, *Helvet. Chim. Acta* **57** (1974), no. 6, 1731–1744. URL `http://onlinelibrary.wiley.com/doi/abs/10.1002/hlca.19740570625`.

[51] Kohn W. and Sham L. J., Self-consistent equations including exchange and correlation effects, *Phys. Rev.* **140** (1965), A1133–A1138. URL `http://link.aps.org/doi/10.1103/PhysRev.140.A1133`.

[52] Lee C., Yang W., and Parr R. G., Development of the Colle-Salvetti correlation-energy formula into a functional of the electron density, *Phys. Rev. B* **37** (1988), 785–789. URL `https://link.aps.org/doi/10.1103/PhysRevB.37.785`.

[53] Li P., Dft studies on configurations, stabilities, and ir spectra of neutral carbon clusters, *J. At. Mol. Sci.* **3** (2012), no. 4, 308–322. URL `http://global-sci.org/intro/article_detail/jams/8211.html`.

[54] Liao M.-S. and Scheiner S., Electronic structure and bonding in metal porphyrins, metal=Fe, Co, Ni, Cu, Zn, *J. Chem. Phys.* **117** (2002), no. 1, 205–219. URL `http://doi.org/10.1063/1.1480872`.

[55] Littlewood D. E., Richardson A. R., and Turnbull H. W., Group characters and algebra, *Philos. Trans. Roy. Soc. London A* **233** (1934), no. 721-730, 99–141. URL `http://royalsocietypublishing.org/doi/abs/10.1098/rsta.1934.0015`.

[56] Liu J. et al., Quantum algorithms for electronic structures: basis sets and boundary conditions, *Chem. Soc. Rev.* **51** (2022), 3263–3279. URL `http://dx.doi.org/10.1039/D1CS01184G`.

[57] Lynch B. J., Zhao Y., and Truhlar D. G., Effectiveness of diffuse basis functions for calculating relative energies by density functional theory, *J. Phys. Chem. A* **107** (2003), no. 9, 1384–1388. URL `http://doi.org/10.1021/jp0215901`.

[58] MathWorks Inc., Matlab (version 2021a), Computer Software, 2021. URL `http://www.mathworks.com`.

[59] Mulliken R. S., Electronic structures of polyatomic molecules and valence. iv. electronic states, quantum theory of the double bond, *Phys. Rev.* **43** (1933), 279–302. URL `http://doi.org/10.1103/PhysRev.43.279`.

[60] Paier J., Marsman M., and Kresse G., Why does the B3LYP hybrid functional fail for metals?, *J. Chem. Phys.* **127** (2007), no. 2, 024103. URL `https://doi.org/10.1063/1.2747249`.

[61] Parasuk V. and Almlöf J., The electronic and molecular structure of carbon clusters: C_8 and C_{10}, *Theor. Chim. Acta* **83** (1992), no. 3, 227–237. URL `http://doi.org/10.1007/BF01132831`.

[62] Perdew J. P., Density-functional approximation for the correlation energy of the inhomogeneous electron gas, *Phys. Rev. B* **33** (1986), 8822–8824. URL `http://link.aps.org/doi/10.1103/PhysRevB.33.8822`.

[63] Pino T. et al., Electronic spectra of the chains $HC_{2n}H$ ($n = 8-13$) in the gas phase, *J. Chem. Phys.* **114** (2001), no. 5, 2208–2212.

[64] Pinsky M., Lipkowitz K. B., and Avnir D., Continuous symmetry measures. VI. The relations between polyhedral point-group/subgroup symmetries, *J. Math. Chem.* **30** (2001), no. 1, 109–120. URL `http://doi.org/10.1023/A:1013133602531`.

[65] Raghavachari K., Whiteside R. A., and Pople J. A., Structures of small carbon clusters: Cyclic ground state of C_6, *J. Chem. Phys.* **85** (1986), no. 11, 6623–6628. URL `http://doi.org/10.1063/1.451444`.

[66] Remya K. and Suresh C. H., Carbon rings: a DFT study on geometry, aromaticity, intermolecular carbon–carbon interactions and stability, *RSC Adv.* **6** (2016), 44261–44271. URL `http://doi.org/10.1039/C6RA06833B`.

[67] Rothenberg S. and Schaefer, H. F. I., Methane as a numerical experiment for polarization basis function selection, *J. Chem. Phys.* **54** (2003), no. 6, 2764–2766. URL `http://doi.org/10.1063/1.1675248`.

[68] Safarowsky O. et al., Nomenclature for catenanes, rotaxanes, molecular knots, and assemblies derived from these structural elements, *J. Prakt. Chem.* **342** (2000), no. 5, 437–444.

[69] Schrödinger E., An undulatory theory of the mechanics of atoms and molecules, *Phys. Rev.* **28** (1926), 1049–1070. URL `http://link.aps.org/doi/10.1103/PhysRev.28.1049`.

[70] Sestraş R., Jäntschi L., and Bolboacă S., Quantum mechanics study on a series of steroids relating separation with structure, *JPC J. Planar Chromat.* **25** (2012), no. 6, 528 – 533. URL `http://akjournals.com/view/journals/1006/25/6/article-p528.xml`.

[71] Setsune J.-i. et al., Synthesis, structure, and magnetic properties of linear trinuclear Cu^{II} and Ni^{II} complexes of porphyrin analogues embedded with binaphthol units, *Symmetry* **12** (2020), no. 10, 1610. URL `http://doi.org/10.3390/sym12101610`.

[72] Slater J. C., The theory of complex spectra, *Phys. Rev.* **34** (1929), 1293–1322. URL `http://link.aps.org/doi/10.1103/PhysRev.34.1293`.

[73] Slater J. C., Atomic shielding constants, *Phys. Rev.* **36** (1930), 57–64. URL `http://link.aps.org/doi/10.1103/PhysRev.36.57`.

[74] Sloane N. J. A., A000602. number of n-node unrooted quartic trees; number of n-carbon alkanes $C(n)H(2n+2)$ ignoring stereoisomers, The On-Line Encyclopedia of Integer Sequences, 2023. URL `http://oeis.org/A000602`.

[75] Sloane N. J. A., A000628. number of n-node unrooted steric quartic trees; number of n-carbon alkanes $C(n)H(2n+2)$ taking stereoisomers into account, The On-Line Encyclopedia of Integer Sequences, 2023. URL `http://oeis.org/A000628`.

[76] Springborg M. and Kavan L., On the stability of polyyne, *Chem. Phys.* **168** (1992), no. 2, 249–258. URL `http://sciencedirect.com/science/article/pii/0301010492871597`.

[77] Springborg M. and Kavan L., Can linear carbon chains be synthesized?, *Synth. Met.* **57** (1993), no. 2, 4405–4410. URL `http://sciencedirect.com/science/article/pii/037967799390757N`.

[78] Stephens P. J. et al., Theoretical calculation of vibrational circular dichroism spectra, *Faraday Discuss.* **99** (1994), 103–119. URL `http://doi.org/10.1039/FD9949900103`.

[79] Stoenoiu C. E., Putz M. V., and Jäntschi L., Is triple crossed C_{28} cyclic polyyne cluster a stable conformation?, *Fullerenes, Nanotubes and Carbon Nanostructures* **32** (2024), no. 1, 55–67. URL `http://doi.org/10.1080/1536383X.2023.2261573`.

[80] Straka M., Patzschke M., and Pyykkö P., Why are hexavalent uranium cyanides rare while U-F and U-O bonds are common and short?, *Theor. Chem. Acc.* **109** (2003), no. 6, 332–340. URL `http://doi.org/10.1007/s00214-003-0441-7`.

[81] Wang Z. et al., A new carbon solid made of the world's smallest caged fullerene C_{20}, *Phys. Lett. A* **280** (2001), no. 5, 351–356. URL `http://sciencedirect.com/science/article/pii/S0375960100008471`.

[82] Wavefunction I., *Tutorial and User's Guide*, Elsevier, Irvine, CA, U.S.A., 2019. URL `http://downloads.wavefun.com/FAQ/Spartan18Manual.pdf`.

[83] Wolinski K., Hinton J. F., and Pulay P., Efficient implementation of the gauge-independent atomic orbital method for NMR chemical shift calculations, *J. Am. Chem. Soc.* **112** (1990), no. 23, 8251–8260. URL `http://doi.org/10.1021/ja00179a005`.

[84] Yanai T., Tew D. P., and Handy N. C., A new hybrid exchange–correlation functional using the coulomb-attenuating method (cam-b3lyp), *Chem. Phys. Lett.* **393** (2004), no. 1, 51–57. URL `http://www.sciencedirect.com/science/article/pii/S0009261404008620`.

[85] Zhang Q. L. et al., Reactivity of large carbon clusters: spheroidal carbon shells and their possible relevance to the formation and morphology of soot, *J. Phys. Chem.* **90** (1986), no. 4, 525–528. URL `http://doi.org/10.1021/j100276a001`.

[1] DEPARTMENT OF PHYSICS AND CHEMISTRY, TECHNICAL UNIVERSITY OF CLUJ-NAPOCA
Email address: `lorentz.jantschi@chem.utcluj.ro`

[2] DEPARTMENT OF CHEMISTRY AND BIOLOGY, TECHNICAL UNIVERSITY OF CLUJ-NAPOCA
Email address: `lavinia.pruteanu@cb.utcluj.ro`